

# HIGHLY EFFICIENT AND ENERGY DISSIPATIVE SCHEMES FOR THE TIME FRACTIONAL ALLEN-CAHN EQUATION\*

DIANMING HOU<sup>1</sup> CHUANJU XU<sup>2,3</sup>

**ABSTRACT.** In this paper, we propose and analyze a time-stepping method for the time fractional Allen-Cahn equation. The key property of the proposed method is its unconditional stability for general meshes, including the graded mesh commonly used for this type of equations. The unconditional stability is proved through establishing a discrete nonlocal free energy dissipation law, which is also true for the continuous problem. The main idea used in the analysis is to split the time fractional derivative into two parts: a local part and a history part, which are discretized by the well known L1, L1-CN, and  $L1^+$ -CN schemes. Then an extended auxiliary variable approach is used to deal with the nonlinear and history term. The main contributions of the paper are: First, it is found that the time fractional Allen-Cahn equation is a dissipative system related to a nonlocal free energy. Second, we construct efficient time stepping schemes satisfying the same dissipation law at the discrete level. In particular, we prove that the proposed schemes are unconditionally stable for quite general meshes. Finally, the efficiency of the proposed method is verified by a series of numerical experiments.

## 1. INTRODUCTION

As a class of mathematical models, gradient flows is partial differential equations under the form:

$$\frac{\partial \phi}{\partial t} = -\text{grad}_H E(\phi), \quad (1.1)$$

where  $\phi$  is the state function (also called phase function in many cases),  $E(\cdot)$  is the free energy driving functional associated to the physical problem, and  $\text{grad}_H E(\cdot)$  is the functional derivative of  $E$  in the Sobolev space  $H$ . It has other names: it is often called variational principle in mathematics and Onsager principle in physics. Obviously the gradient flows satisfies the energy dissipation law:

$$\frac{d}{dt} E(\phi) = \left( \text{grad}_H E(\phi), \frac{\partial \phi}{\partial t} \right) = -\left\| \frac{\partial \phi}{\partial t} \right\|_0^2, \quad (1.2)$$

---

*Date:* April 27, 2021.

*2020 Mathematics Subject Classification.* 65N35, 65M70, 45K05, 41A05, 41A10, 41A25.

*Key words and phrases.* time fractional Allen-Cahn, time-stepping scheme, unconditional stability, spectral method.

\*The work of D. Hou is supported by NSFC grant 12001248 and the Natural Science Foundation of the Jiangsu Higher Education Institutions of China grant BK20201020. The second author has received support from NSFC grant 11971408, NNW2018-ZT4A06 project, and NSFC/ANR joint program 51661135011/ANR-16-CE40-0026-01.

<sup>1</sup>School of Mathematics and Statistics, Jiangsu Normal University, 221116 Xuzhou, China.

<sup>2</sup>School of Mathematical Sciences and Fujian Provincial Key Laboratory of Mathematical Modeling and High Performance Scientific Computing, Xiamen University, 361005 Xiamen, China.

<sup>3</sup>Corresponding author. Email: cjxu@xmu.edu.cn (C. Xu).

where  $(\cdot, \cdot)$  and  $\|\cdot\|_0$  stand for the  $L^2(\Omega)$ -inner product and norm, respectively. This means that the state function  $\phi$  evolves in such a way that the energy functional  $E$  dissipates in time, i.e., in the opposite direction to the gradient of  $E$  at  $\phi$ . This makes the models very useful in many fields of science and engineering, such as interface dynamics [4, 5, 18, 40], thin films [17, 30], crystal growth [12–14], polymers [15, 16] and liquid crystals [9, 24–26].

In this paper, we are interested in the following model:

$${}_0D_t^\alpha \phi = -\text{grad}_H E(\phi), \quad (1.3)$$

deriving from gradient flows having a modified dissipation mechanism. Here  $0 < \alpha < 1$ ,  ${}_0D_t^\alpha$  is the Caputo fractional derivative defined by

$${}_0D_t^\alpha \phi(t) = \frac{1}{\Gamma(1-\alpha)} \int_0^t (t-s)^{-\alpha} \phi'(s) ds.$$

In mathematics gradient flows involving fractional derivatives have been extensively studied in recent years; see, .e.g, [1–3, 6, 10, 21, 27, 29, 36, 41, 42]. From the definition it is seen that the fractional derivative is some kind of weighted average in the history of the traditional derivative. This means that the change rate, i.e., the derivative, at the current time is affected by the historical rates. In a larger field this property has been found quite useful in describing the memory effect which can be present, for example, in some materials such as viscoelastic materials or polymers. Intuitively, the gradient flows model (1.3) can be used to describe the systems in which dissipation of the associated free energy has memory effect in some circumstances. One of typical examples of such models is the fractional Allen-Cahn equation, which is also the focus of this paper. There exist a number of studies for this equation. Tang et al. [37] proved that the time-fractional phase field model admits an integral type energy dissipation law. They investigated the L1 time stepping scheme on the uniform mesh, which is of first order energy stable accuracy. Du et al. [11] developed several time schemes based on the convex splitting and weighted stabilization, and proved that the convergence rates of their schemes are of order- $\alpha$  in the uniform mesh without regularity assumption on the solution. Recently, Liao et al. [22] proposed an adaptive second-order Crank-Nicolson time-stepping scheme using SAV approach for the time-fractional MBE model, and showed that the proposed scheme are unconditional stable on the nonuniform mesh. Very recently, Quan et al. [31] theoretically proved the time-fractional energy law and the weighted dissipation law. Accordingly, they constructed a first order numerical method on the uniform time mesh [32], which preserved the energy laws. However, it seems not easy to construct higher order schemes for nonuniform meshes satisfying the same energy laws.

The aim of the present paper is to propose easy-to-implement and unconditionally stable schemes, which preserve a non-local energy dissipation law to be specified. The main idea in constructing the schemes is to use existing efficient approximations to discretize the local part and history part of the fractional derivative respectively, and use auxiliary variable approaches [19, 33, 34] to deal with the nonlinear potential in the free energy. The contributions of the paper are threefold:

- Finding of a non-local energy dissipation law of the time fractional gradient flows.
- Construction of several unconditionally stable schemes for the time fractional Allen-Cahn equation, which satisfy a discrete version of the energy dissipation law. It is proved that the stability and energy dissipation law remain true on the graded mesh, which is useful

in recovering the optimal convergence order for typical solutions having low regularity at the initial time.

- The proposed schemes are very easy to implement. That is, only several Poisson-type equations with constant coefficients need to be solved at each time step. Furthermore, a fast evaluation technique based on the sum-of-exponentials approach is used to accelerate the calculation and reduce the storage.

The paper is organized as follows: In the next section, we derive the non-local energy dissipation law for the time fractional gradient flows. In Section 3, we construct and analyze the first order numerical scheme. A discrete energy dissipation law of the scheme is established for general time grids. In Section 4, we propose and analyze two higher order schemes: a  $2 - \alpha$  order and a second order schemes based on Crank-Nicolson formula. The unconditional stability of the both schemes are rigorously proved. The numerical experiments are carried out in Section 5, not only to validate stability and accuracy of the proposed methods, but also to numerically investigate the coarsening dynamics. Finally, the paper ends with some concluding remarks.

## 2. NON-LOCAL ENERGY DISSIPATION LAW

We consider the time fractional gradient flows (1.3) in the bounded domain  $\Omega \in \mathbb{R}^n$  ( $n = 1, 2, 3$ ). When  $\alpha = 1$ , it follows from integrating (1.2) from  $t_e$  to  $t_l$  for any  $0 \leq t_e < t_l$  that:

$$E(\phi(t_l)) - E(\phi(t_e)) = - \int_{t_e}^{t_l} \left\| \frac{\partial \phi(\cdot, s)}{\partial s} \right\|_0^2 ds \leq 0.$$

That is, the free energy  $E(\cdot)$  is decreasing in  $t$ . However, for  $0 < \alpha < 1$ , this energy law does not hold no longer. Instead, the solution of (1.3) satisfies an non-local energy law that we derive below. To see that, we split the fractional derivative into two parts as follows:

$${}_0D_t^\alpha \phi(t) = D_{l,t}^{\alpha, \hat{t}} \phi + D_{h,t}^{\alpha, \hat{t}} \phi, \quad (2.1)$$

where  $0 < \hat{t} < t$ , and the local term  $D_{l,t}^{\alpha, \hat{t}} \phi$  and the history term  $D_{h,t}^{\alpha, \hat{t}} \phi$  are respectively defined by

$$D_{l,t}^{\alpha, \hat{t}} \phi = \frac{1}{\Gamma(1-\alpha)} \int_{\hat{t}}^t (t-s)^{-\alpha} \phi'(s) ds, \quad D_{h,t}^{\alpha, \hat{t}} \phi = \frac{1}{\Gamma(1-\alpha)} \int_0^{\hat{t}} (t-s)^{-\alpha} \phi'(s) ds.$$

Now we introduce the non-local “energy”

$$\bar{E}(\hat{t}, t; \phi) := E(\phi) + F_h(\hat{t}, t; \phi), \quad 0 < \hat{t} < t, \quad (2.2)$$

where  $F_h(\hat{t}, t; \phi)$  is the non-local part of the energy, defined by

$$F_h(\hat{t}, t; \phi) := \int_{\Omega} \int_{\hat{t}}^t D_{h,s}^{\alpha, \hat{t}} \phi \frac{\partial \phi}{\partial s} ds d\mathbf{x}, \quad 0 < \hat{t} < t.$$

A direct calculation shows

$$\frac{d}{dt} \bar{E}(\hat{t}, t; \phi) = \frac{d}{dt} E(\phi) + \left( D_{h,t}^{\alpha, \hat{t}} \phi, \frac{\partial \phi}{\partial t} \right) = \left( \text{grad}_H E(\phi), \frac{\partial \phi}{\partial t} \right) + \left( D_{h,t}^{\alpha, \hat{t}} \phi, \frac{\partial \phi}{\partial t} \right), \quad 0 < \hat{t} < t.$$

Then using (1.3) and (2.1) gives

$$\frac{d}{dt} \bar{E}(\hat{t}, t; \phi) = (-{}_0D_t^\alpha \phi(t), \frac{\partial \phi}{\partial t}) + \left( D_{h,t}^{\alpha, \hat{t}} \phi, \frac{\partial \phi}{\partial t} \right) = - \left( D_{l,t}^{\alpha, \hat{t}} \phi, \frac{\partial \phi}{\partial t} \right), \quad 0 < \hat{t} < t. \quad (2.3)$$

This allows to establish the following “energy” decay property: for  $0 < \hat{t} < t$ , integrating (2.3) yields

$$\overline{E}(\hat{t}, t; \phi(t)) - \overline{E}(\hat{t}, \hat{t}; \phi(\hat{t})) = - \int_{\Omega} \int_{\hat{t}}^t D_{l,s}^{\alpha, \hat{t}} \phi \frac{\partial \phi}{\partial s} ds d\mathbf{x}. \quad (2.4)$$

Let's define the bilinear form  $\mathcal{A}_{\alpha}^{\hat{t}, t}(\cdot, \cdot)$  with  $0 < \hat{t} < t$  by: for the functions  $\varphi$  and  $\psi$ ,

$$\mathcal{A}_{\alpha}^{\hat{t}, t}(\varphi, \psi) := \frac{1}{\Gamma(1-\alpha)} \int_{\hat{t}}^t \int_{\hat{t}}^s (s-\sigma)^{-\alpha} \varphi(\sigma) \psi(s) d\sigma ds.$$

It has been known; see, e.g., [20, 37], that the bilinear form  $\mathcal{A}_{\alpha}^{\hat{t}, t}(\cdot, \cdot)$  is positive for any  $0 < \hat{t} < t$ . That is, for any  $\psi \in L^2(\hat{t}, t)$  so that the following expression makes sense, it holds:

$$\mathcal{A}_{\alpha}^{\hat{t}, t}(\psi, \psi) \geq 0. \quad (2.5)$$

It then follows from (2.4) and (2.5) that

$$\overline{E}(\hat{t}, t; \phi(t)) - \overline{E}(\hat{t}, \hat{t}; \phi(\hat{t})) = - \int_{\Omega} \mathcal{A}_{\alpha}^{\hat{t}, t}(\partial_t \phi, \partial_t \phi) d\mathbf{x} \leq 0.$$

This can be regarded as an energy law associated to the functional  $\overline{E}(\hat{t}, t; \phi)$  defined in (2.2). However, the inconvenience in using  $\overline{E}(\hat{t}, t; \phi)$  is that it depends on  $\hat{t}$ , which makes the functional discontinuous in  $t$ . For the numerical purpose it is desirable to derive a continuous-in-time energy, which is dissipative in a given time grid, so that we have a clear goal to construct our numerical scheme satisfying the same dissipation law. To this end, for a given time mesh, say  $0 = t_0 < t_1 < t_2 < \dots < t_M = T$ , we define a new non-local “energy” functional as follows:

$$\overline{E}(\phi) = \begin{cases} E(\phi), & t \in [t_0, t_1], \\ E(\phi) + F_h(t_1, t; \phi), & t \in [t_1, t_2], \\ E(\phi) + F_h(t_n, t; \phi) + \sum_{k=1}^{n-1} F_h(t_k, t_{k+1}; \phi), & t \in [t_n, t_{n+1}], n = 2, \dots, M-1. \end{cases} \quad (2.6)$$

It is readily seen that

$$\frac{d}{dt} \overline{E}(\phi) = - \left( D_{l,t}^{\alpha, t_n} \phi, \frac{\partial \phi}{\partial t} \right), \quad t \in [t_n, t_{n+1}], n = 0, 1, \dots, M-1.$$

Integrating the above equality in the interval  $[t_n, t_{n+1}], n = 0, 1, \dots, M-1$  gives

$$\overline{E}(\phi(t_{n+1})) - \overline{E}(\phi(t_n)) = - \int_{\Omega} \mathcal{A}_{\alpha}^{t_n, t_{n+1}}(\phi_t, \phi_t) d\mathbf{x} \leq 0, \quad \text{for all } n = 0, 1, \dots, M-1. \quad (2.7)$$

We see that for any given time mesh  $\{t_n\}_{n=0}^M$ , the corresponding non-local free energy, defined in (2.6) is dissipative at the grid points. We would like to point out that the functionals defined in (2.2) and (2.6) do not necessarily have any physical meaning. The motivation for introducing such a modified “energy” is purely mathematical. That is, we want to find suitable functionals related to the equation, which decay in time. This provides insight into how a stable scheme should look like. Our aim in the next section is to construct numerical schemes that satisfy the same dissipation law.

## 3. NUMERICAL METHODS — A FIRST ORDER SCHEME

To simplify the presentation, we will only consider the time fractional Allen-Cahn equation, i.e.,

$${}_0D_t^\alpha \phi = -\text{grad}_H E(\phi), \quad (3.1)$$

subject to the periodic boundary condition or Neumann boundary condition, where the free energy  $E(\cdot)$  is defined by

$$E(\phi) := \int_{\Omega} \left[ \frac{\varepsilon^2}{2} |\nabla \phi|^2 + F(\phi) \right] d\mathbf{x}, \quad (3.2)$$

and  $F(\cdot)$  is a nonlinear potential.  $H := L^2(\Omega)$ .

**Auxiliary variable approach.** The proposed schemes are based on a reformulation of the time fractional Allen-Cahn equation by introducing an auxiliary variable — an approach intensively studied recently for gradient flows; see, e.g., [19, 35] and the references therein. The key to is to rewrite the original equation (3.1)-(3.2) into the following equivalent form:

$${}_0D_t^\alpha \phi - \varepsilon^2 \Delta \phi + \left(1 - \frac{R(t)}{R(t)}\right) \theta^2 \Delta \phi + \frac{R(t)}{R(t)} F'(\phi) = 0, \quad (3.3)$$

where

$$R(t) = \sqrt{\bar{E}_\theta(\phi) + C_0}, \quad \theta^2 \leq \varepsilon^2, \quad (3.4)$$

and, for the time grid  $\{t_n\}_0^M$ ,  $\bar{E}_\theta(\phi)$  is defined by

$$\bar{E}_\theta(\phi) = \begin{cases} E_\theta(\phi), & t \in [t_0, t_1], \\ E_\theta(\phi) + F_h(t_1, t; \phi), & t \in [t_1, t_2], \\ E_\theta(\phi) + F_h(t_n, t; \phi) + \sum_{k=1}^{n-1} F_h(t_k, t_{k+1}; \phi), & t \in [t_n, t_{n+1}], n = 2, \dots, M-1, \end{cases}$$

with  $E_\theta(\phi) := \int_{\Omega} \left[ \frac{\theta^2}{2} |\nabla \phi|^2 + F(\phi) \right] d\mathbf{x}$ , and  $C_0$  being a constant such that  $\bar{E}_\theta(\phi) + C_0 > 0$ .

To find a suitable way to discretize the auxiliary variable  $R(t)$ , we take the derivative of (3.4) with respect to  $t$  to obtain the auxiliary equation:

$$\frac{dR}{dt} = \frac{1}{2R(t)} \left( -\theta^2 \Delta \phi + F'(\phi) + D_{h,t}^{\alpha, t_n} \phi, \frac{\partial \phi}{\partial t} \right), \quad \forall t \in [t_n, t_{n+1}], n = 2, \dots, M-1. \quad (3.5)$$

Furthermore, we use the operator splitting (2.1) to rewrite the equation (3.3) under the equivalent form: for  $n = 2, \dots, M-1$ ,

$$D_{l,t}^{\alpha, t_n} \phi - \varepsilon^2 \Delta \phi + \left(1 - \frac{R(t)}{R(t)}\right) \theta^2 \Delta \phi + \frac{R(t)}{R(t)} (F'(\phi) + D_{h,t}^{\alpha, t_n} \phi) = 0, \quad \forall t \in [t_n, t_{n+1}]. \quad (3.6)$$

Now we are led to discretize the equations (3.6) and (3.5). The great advantage of this approach is that, although we have one more variable and one more equation to discretize compared to the original equation, constructing stable and efficient schemes with help of the auxiliary variable turns out to be a much easier task.

Before describing our schemes, we first realize, by taking  $L^2(\Omega)$ -inner products and integrating from  $t_n$  to  $t_{n+1}$  of (3.6) and (3.5) with  $\frac{\partial \phi}{\partial t}$  and  $2R(t)$  respectively, that

$$\left[ R^2(t_{n+1}) + \frac{\varepsilon^2 - \theta^2}{2} \|\nabla \phi(\cdot, t_{n+1})\|_0^2 \right] - \left[ R^2(t_n) + \frac{\varepsilon^2 - \theta^2}{2} \|\nabla \phi(\cdot, t_n)\|_0^2 \right] = - \int_{\Omega} \mathcal{A}_{\alpha}^{t_n, t_{n+1}}(\phi_t, \phi_t) d\mathbf{x} \leq 0. \quad (3.7)$$

Noticing

$$R^2 + \frac{\varepsilon^2 - \theta^2}{2} \|\nabla \phi\|_0^2 = \overline{E}(\phi) + C_0,$$

with  $\overline{E}(\cdot)$  being the non-local energy functional defined in (2.6), we have

$$\overline{E}(\phi(t_{n+1})) - \overline{E}(\phi(t_n)) \leq 0. \quad (3.8)$$

This is exactly the same dissipation law as (2.7), derived from the original equation without the auxiliary variable. We will see that after discretization, the discrete solution satisfies a discrete dissipation law under the form (3.7) rather than (3.8).

Starting with the equivalent equations (3.5) and (3.6), we are now in a position to construct various efficient time stepping schemes to calculate the solution  $\phi$ .

**A first order scheme.** Let  $\tau_n = t_n - t_{n-1}, n = 1, \dots, M$  be the time step size, and  $\tau = \max\{\tau_n, n = 1, \dots, M\}$  be the maximum step size.

We propose to use the popular L1 approximation [28] to discretize the local and history parts of the Caputo fractional derivative at  $t = t_{n+1}$ :

$$\begin{aligned} D_{l, t_{n+1}}^{\alpha, t_n} \phi &= \frac{1}{\Gamma(1-\alpha)} \int_{t_n}^{t_{n+1}} (t_{n+1} - s)^{-\alpha} \phi_s(s) ds \\ &= \frac{1}{\Gamma(1-\alpha)} \frac{\phi(t_{n+1}) - \phi(t_n)}{\tau_{n+1}} \int_{t_n}^{t_{n+1}} (t_{n+1} - s)^{-\alpha} ds + e_{l, \tau}^{n+1} \\ &:= L_l^{\alpha} \phi(t_{n+1}) + e_{l, \tau}^{n+1}, \\ D_{h, t_{n+1}}^{\alpha, t_n} \phi &= \frac{1}{\Gamma(1-\alpha)} \sum_{k=0}^{n-1} \int_{t_k}^{t_{k+1}} (t_{n+1} - s)^{-\alpha} \phi_s(s) ds \\ &= \sum_{k=0}^{n-1} \frac{1}{\Gamma(1-\alpha)} \frac{\phi(t_{k+1}) - \phi(t_k)}{\tau_{k+1}} \int_{t_k}^{t_{k+1}} (t_{n+1} - s)^{-\alpha} ds + e_{h, \tau}^{n+1} \\ &:= L_h^{\alpha} \phi(t_{n+1}) + e_{h, \tau}^{n+1}, \end{aligned}$$

where the discrete fractional operators  $L_l^{\alpha}$  and  $L_h^{\alpha}$  are defined respectively by

$$\begin{aligned} L_l^{\alpha} \phi(t_{n+1}) &= b_0 \frac{\phi(t_{n+1}) - \phi(t_n)}{\tau_{n+1}}, \\ L_h^{\alpha} \phi(t_{n+1}) &= \sum_{k=0}^{n-1} b_{n-k} \frac{\phi(t_{k+1}) - \phi(t_k)}{\tau_{k+1}}, \end{aligned}$$

and the coefficients  $b_k$  are given by

$$b_{n-k} = \frac{1}{\Gamma(1-\alpha)} \int_{t_k}^{t_{k+1}} (t_{n+1} - s)^{-\alpha} ds > 0, k = 0, 1, \dots, n.$$

The truncation errors  $e_{l,\tau}^{n+1}$  and  $e_{h,\tau}^{n+1}$  are defined respectively by

$$e_{l,\tau}^{n+1} = \frac{1}{\Gamma(1-\alpha)} \left[ \int_{t_n}^{t_{n+1}} (t_{n+1}-s)^{-\alpha} \phi_s(s) ds - \frac{\phi(t_{n+1}) - \phi(t_n)}{\tau_{n+1}} \int_{t_n}^{t_{n+1}} (t_{n+1}-s)^{-\alpha} ds \right],$$

and

$$e_{h,\tau}^{n+1} = \frac{1}{\Gamma(1-\alpha)} \left[ \int_0^{t_n} (t_{n+1}-s)^{-\alpha} \phi_s(s) ds - \sum_{k=0}^{n-1} \frac{\phi(t_{k+1}) - \phi(t_k)}{\tau_{k+1}} \int_{t_k}^{t_{k+1}} (t_{n+1}-s)^{-\alpha} ds \right].$$

For the graded mesh, i.e.,  $t_n = \left(\frac{n}{M}\right)^r T$ ,  $r \geq 1$ ,  $n = 0, 1, \dots, M$ , which is particularly interesting for this problem and also the focus of this paper, a direct calculation gives

$$b_j = \frac{T^{1-\alpha}}{\Gamma(2-\alpha)M^{(1-\alpha)r}} \left[ ((n+1)^r - (n-j)^r)^{1-\alpha} - ((n+1)^r - (n-j+1)^r)^{1-\alpha} \right].$$

Noting that when  $r = 1$ , it is the uniform mesh.

It can be proved [20, 28] that the truncation error  $e_{l,\tau}^{n+1}$  and  $e_{h,\tau}^{n+1}$  can be bounded by  $c_\phi \tau^{2-\alpha}$ , where  $c_\phi$  is a positive constant depending on the regularity of  $\phi$ .

The above approximation motivates us to consider the following scheme for (3.6) and (3.5):

$$L_l^\alpha \phi^{n+1} - \varepsilon^2 \Delta \phi^{n+1} + \left(1 - \frac{R^{n+1}}{R^n}\right) \theta^2 \Delta \phi^n + \frac{R^{n+1}}{R^n} (F'(\phi^n) + L_h^\alpha \phi^{n+1}) = 0, \quad (3.9a)$$

$$\frac{R^{n+1} - R^n}{\tau_{n+1}} = \frac{1}{2R^n} \left( -\theta^2 \Delta \phi^n + F'(\phi^n) + L_h^\alpha \phi^{n+1}, \frac{\phi^{n+1} - \phi^n}{\tau_{n+1}} \right), \quad (3.9b)$$

where  $\phi^n$  is an approximation to  $\phi(t_n)$ . Intuitively, this is a first order scheme since it is a combination of some approximations of first order and  $2 - \alpha$  order to different terms of the equations. However a rigorous proof of the convergence order remains an open question. Instead, we will provide a proof for the stability of the scheme, and the convergence order will be verified through the numerical experiments to be presented later on.

**Stability.** The stability property of the first order scheme (3.9) is presented and proved in the following theorem.

**Theorem 3.1.** *Without any restriction on the mesh, the scheme (3.9) is stable in the sense that the following discrete energy dissipation law holds*

$$E_{\varepsilon,\theta}^{n+1} - E_{\varepsilon,\theta}^n \leq 0, \quad n = 0, 1, \dots,$$

where

$$E_{\varepsilon,\theta}^n := \frac{1}{2} (\varepsilon^2 - \theta^2) \|\nabla \phi^n\|_0^2 + |R^n|^2, \quad \theta^2 \leq \varepsilon^2.$$

*Proof.* First, taking the  $L^2$ -inner products of (3.9a) and (3.9b) with  $\phi^{n+1} - \phi^n$  and  $2R^{n+1}$  respectively, we obtain:

$$\begin{aligned} & (L_l^\alpha \phi^{n+1}, \phi^{n+1} - \phi^n) + (\varepsilon^2 - \theta^2) (\nabla \phi^{n+1}, \nabla (\phi^{n+1} - \phi^n)) + \theta^2 \|\nabla (\phi^{n+1} - \phi^n)\|_0^2 \\ & \quad + \frac{R^{n+1}}{R^n} (-\theta^2 \Delta \phi^n + F'(\phi^n) + L_h^\alpha \phi^{n+1}), \phi^{n+1} - \phi^n = 0, \\ & 2R^{n+1} (R^{n+1} - R^n) = \frac{R^{n+1}}{R^n} (-\theta^2 \Delta \phi^n + F'(\phi^n) + L_h^\alpha \phi^{n+1}, \phi^{n+1} - \phi^n). \end{aligned}$$

Then combining these two equalities, using the identity

$$2a^{n+1}(a^{n+1} - a^n) = |a^{n+1}|^2 - |a^n|^2 + |a^{n+1} - a^n|^2,$$

and dropping some non-essential positive terms, we obtain

$$E_{\varepsilon, \theta}^{n+1} - E_{\varepsilon, \theta}^n \leq -(L_l^\alpha \phi^{n+1}, \phi^{n+1} - \phi^n) = -\frac{b_0}{\tau_{n+1}} \|\phi^{n+1} - \phi^n\|_0^2 \leq 0, \quad n = 0, 1, 2, \dots,$$

This ends the proof.  $\square$

**Implementation.** Beside of its unconditional stability proved in Theorem 3.1, another notable property of the scheme (3.9) is that it can be efficiently implemented. To see that, we first eliminate  $R^{n+1}$  from (3.9a) by using (3.9b) to obtain

$$b_0 \frac{\phi^{n+1} - \phi^n}{\tau_{n+1}} - \varepsilon^2 \Delta \phi^{n+1} + \theta^2 \Delta \phi^n + \left[ 1 + \frac{1}{2|R^n|^2} (\gamma^n, \phi^{n+1} - \phi^n) \right] \gamma^n = 0, \quad (3.10)$$

where

$$\gamma^n := -\theta^2 \Delta \phi^n + F'(\phi^n) + L_h^\alpha \phi^{n+1}.$$

Then reformulating (3.10) gives

$$\left( \frac{b_0}{\tau_{n+1}} I_d - \varepsilon^2 \Delta \right) \phi^{n+1} + (\gamma^n, \phi^{n+1}) \frac{\gamma^n}{2|R^n|^2} = \frac{b_0}{\tau_{n+1}} \phi^n - \theta^2 \Delta \phi^n - \left[ \frac{R^n}{R^n} - \frac{1}{2|R^n|^2} (\gamma^n, \phi^n) \right] \gamma^n. \quad (3.11)$$

Denoting the right hand side of (3.11) by  $g(\phi^n)$ , we see that the problem (3.11) can be solved in two steps as follows:

$$\begin{cases} \left( \frac{b_0}{\tau_{n+1}} I_d - \varepsilon^2 \Delta \right) \phi_1^{n+1} = -\frac{\gamma^n}{2|R^n|^2}, \\ \text{Neumann boundary condition or periodic boundary condition on } \phi_1^{n+1}; \end{cases} \quad (3.12a)$$

$$\begin{cases} \left( \frac{b_0}{\tau_{n+1}} I_d - \varepsilon^2 \Delta \right) \phi_2^{n+1} = g(\phi^n), \\ \text{Neumann boundary condition or periodic boundary condition on } \phi_2^{n+1}; \end{cases} \quad (3.12b)$$

$$\phi^{n+1} = (\gamma^n, \phi^{n+1}) \phi_1^{n+1} + \phi_2^{n+1}. \quad (3.12c)$$

In a first look it seems that (3.12c) governing the unknown  $\phi^{n+1}$  is an implicit equation. However a careful examination shows that  $(\gamma^n, \phi^{n+1})$  in (3.12c) can be determined explicitly. In fact, taking the inner product of (3.12c) with  $\gamma^n$  yields

$$(\gamma^n, \phi^{n+1}) + \sigma^n (\gamma^n, \phi^{n+1}) = (\gamma^n, \phi_2^{n+1}), \quad (3.13)$$

where

$$\sigma^n = -(\gamma^n, \phi_1^{n+1}) = \left( \gamma^n, A^{-1} \frac{\gamma^n}{2|R^n|^2} \right) \quad \text{with } A = \frac{b_0}{\tau_{n+1}} I_d - \varepsilon^2 \Delta.$$

Note that  $A^{-1}$  is a positive definite operator. Thus  $\sigma^n \geq 0$ . Then it follows from (3.13) that

$$(\gamma^n, \phi^{n+1}) = \frac{(\gamma^n, \phi_2^{n+1})}{1 + \sigma^n}. \quad (3.14)$$

Using this expression,  $\phi^{n+1}$  can be explicitly computed from (3.12c).

In detail, the scheme (3.9) results in the following algorithm at each time step:

(i) Calculation of  $\phi_1^{n+1}$  and  $\phi_2^{n+1}$ : solving the elliptic problems (3.12a) and (3.12b) respectively, which can be realized in parallel.

(ii) Evaluation of  $(\gamma^n, \phi^{n+1})$  using (3.14), then  $\phi^{n+1}$  using (3.12c).

Thus the overall computational cost at each time step comes essentially from solving two second-order elliptic problems with constant coefficients, for which there exist different fast solvers depending on the spatial discretization method.

#### 4. HIGHER ORDER SCHEMES

**4.1. A  $2 - \alpha$  order scheme.** Using L1-CN formula [20] to discrete both the local and history parts of the fractional derivative at  $t = t_{n+\frac{1}{2}} := \frac{t_n+t_{n+1}}{2}$  gives

$$\begin{aligned} D_{l,t_{n+\frac{1}{2}}}^{\alpha,t_n} \phi &= \frac{1}{\Gamma(1-\alpha)} \int_{t_n}^{t_{n+\frac{1}{2}}} (t_{n+\frac{1}{2}} - s)^{-\alpha} \phi_s(s) ds \\ &= \frac{1}{\Gamma(1-\alpha)} \frac{\phi(t_{n+1}) - \phi(t_n)}{\tau_{n+1}} \int_{t_n}^{t_{n+\frac{1}{2}}} (t_{n+1} - s)^{-\alpha} ds + e_{l,\tau}^{n+\frac{1}{2}} \\ &:= \tilde{L}_l^\alpha \phi(t_{n+\frac{1}{2}}) + e_{l,\tau}^{n+\frac{1}{2}}, \end{aligned}$$

$$\begin{aligned} D_{h,t_{n+\frac{1}{2}}}^{\alpha,t_n} \phi &= \frac{1}{\Gamma(1-\alpha)} \sum_{k=0}^{n-1} \int_{t_k}^{t_{k+1}} (t_{n+\frac{1}{2}} - s)^{-\alpha} \phi_s(s) ds \\ &= \sum_{k=0}^{n-1} \frac{1}{\Gamma(1-\alpha)} \frac{\phi(t_{k+1}) - \phi(t_k)}{\tau_{k+1}} \int_{t_k}^{t_{k+1}} (t_{n+\frac{1}{2}} - s)^{-\alpha} ds + e_{h,\tau}^{n+\frac{1}{2}} \\ &:= \tilde{L}_h^\alpha \phi(t_{n+\frac{1}{2}}) + e_{h,\tau}^{n+\frac{1}{2}}, \end{aligned}$$

where the L1-CN difference operators  $\tilde{L}_l^\alpha$  and  $\tilde{L}_h^\alpha$  are defined respectively by

$$\tilde{L}_l^\alpha \phi(t_{n+\frac{1}{2}}) = \tilde{b}_0 \frac{\phi(t_{n+1}) - \phi(t_n)}{\tau_{n+1}}, \quad \tilde{L}_h^\alpha \phi(t_{n+\frac{1}{2}}) = \sum_{k=0}^{n-1} \tilde{b}_{n-k} \frac{\phi(t_{k+1}) - \phi(t_k)}{\tau_{k+1}},$$

with

$$\tilde{b}_0 = \frac{\tau_{n+1}^{1-\alpha}}{\Gamma(2-\alpha)2^{1-\alpha}} > 0, \quad \tilde{b}_{n-k} = \frac{1}{\Gamma(1-\alpha)} \int_{t_k}^{t_{k+1}} (t_{n+\frac{1}{2}} - s)^{-\alpha} ds > 0, \quad k = 0, 1, \dots, n-1.$$

The corresponding truncation errors  $e_{l,\tau}^{n+1}$  and  $e_{h,\tau}^{n+1}$  are defined respectively by

$$e_{l,\tau}^{n+\frac{1}{2}} = \frac{1}{\Gamma(1-\alpha)} \left[ \int_{t_n}^{t_{n+\frac{1}{2}}} (t_{n+\frac{1}{2}} - s)^{-\alpha} \phi_s(s) ds - \frac{\phi(t_{n+1}) - \phi(t_n)}{\tau_{n+1}} \int_{t_n}^{t_{n+\frac{1}{2}}} (t_{n+\frac{1}{2}} - s)^{-\alpha} ds \right],$$

and

$$e_{h,\tau}^{n+\frac{1}{2}} = \frac{1}{\Gamma(1-\alpha)} \left[ \int_0^{t_n} (t_{n+\frac{1}{2}} - s)^{-\alpha} \phi_s(s) ds - \sum_{k=0}^{n-1} \frac{\phi(t_{k+1}) - \phi(t_k)}{\tau_{k+1}} \int_{t_k}^{t_{k+1}} (t_{n+\frac{1}{2}} - s)^{-\alpha} ds \right].$$

It has been proved [20] that the truncation error  $e_{l,\tau}^{n+1}$  and  $e_{h,\tau}^{n+1}$  are both of  $2 - \alpha$  order with respect to  $\tau$ .

Applying the difference operators  $\tilde{L}_l^\alpha$  and  $\tilde{L}_h^\alpha$  to discretize the fractional derivative and the Crank-Nicolson scheme to the remaining terms of the system (3.5) and (3.6), we obtain L1-CN scheme as follows:

$$\begin{aligned} \tilde{L}_l^\alpha \phi^{n+\frac{1}{2}} - \varepsilon^2 \frac{\Delta(\phi^{n+1} + \phi^n)}{2} + \left(1 - \frac{R^{n+1} + R^n}{2R^{n+\frac{1}{2}}}\right) \theta^2 \Delta \phi^{n+\frac{1}{2}} \\ + \frac{R^{n+1} + R^n}{2R^{n+\frac{1}{2}}} \left(F'(\phi^{n+\frac{1}{2}}) + \tilde{L}_h^\alpha \phi^{n+\frac{1}{2}}\right), \end{aligned} \quad (4.1a)$$

$$\frac{R^{n+1} - R^n}{\tau_{n+1}} = \frac{1}{2R^{n+\frac{1}{2}}} \left(-\theta^2 \Delta \phi^{n+\frac{1}{2}} + F'(\phi^{n+\frac{1}{2}}) + \tilde{L}_h^\alpha \phi^{n+\frac{1}{2}}, \frac{\phi^{n+1} - \phi^n}{\tau_{n+1}}\right), \quad (4.1b)$$

where  $\phi^{n+\frac{1}{2}} := \phi^n + \frac{\tau_{n+1}}{2\tau_n}[\phi^n - \phi^{n-1}]$  and  $R^{n+\frac{1}{2}} := R^n + \frac{\tau_{n+1}}{2\tau_n}[R^n - R^{n-1}]$  are the explicit approximation to  $\phi(t_{n+\frac{1}{2}})$  and  $R(t_{n+\frac{1}{2}})$ , respectively.

The scheme (4.1) is expected to have  $2-\alpha$  order convergence, since formally the approximation to the fractional derivative  ${}_0D_{t_{n+\frac{1}{2}}}^\alpha \phi$  is of  $2-\alpha$  order, and the remaining approximations are based on the Crank-Nicolson formula, which is second-order accurate.

The unconditional stability of the L1-CN scheme (4.1) is proved in the following theorem.

**Theorem 4.1.** *The L1-CN scheme (4.1) satisfies the energy law:*

$$\begin{aligned} \frac{\varepsilon^2 - \theta^2}{2} \|\nabla \phi^{n+1}\|_0^2 + \frac{\theta^2}{4} \|\nabla(\phi^{n+1} - \phi^n)\|_0^2 + |R^{n+1}|^2 \\ - \left[ \frac{\varepsilon^2 - \theta^2}{2} \|\nabla \phi^n\|_0^2 + \frac{\theta^2}{4} \left(\frac{\tau_{n+1}}{\tau_n}\right)^2 \|\nabla(\phi^n - \phi^{n-1})\|_0^2 + |R^n|^2 \right] \leq 0, \quad n = 0, 1, \dots \end{aligned}$$

Therefore, the scheme (4.1) is unconditionally stable when i) the mesh is uniform, i.e.,  $\frac{\tau_{n+1}}{\tau_n} = 1$ ; ii)  $\theta = 0$ . In the former case, the discrete energy  $\frac{\varepsilon^2 - \theta^2}{2} \|\nabla \phi^{n+1}\|_0^2 + \frac{\theta^2}{4} \|\nabla(\phi^{n+1} - \phi^n)\|_0^2 + |R^{n+1}|^2$  decreases during the time stepping, while in the latter case, the energy  $\tilde{E}_\varepsilon^{n+1} := \frac{\varepsilon^2}{2} \|\nabla \phi^{n+1}\|_0^2 + |R^{n+1}|^2$  decays in time.

*Proof.* By taking the inner products of (4.1a) and (4.1b) with  $\phi^{n+1} - \phi^n$  and  $R^{n+1} + R^n$  respectively, we have

$$\begin{aligned} (\tilde{L}_l^\alpha \phi^{n+\frac{1}{2}}, \phi^{n+1} - \phi^n) + \frac{\varepsilon^2 - \theta^2}{2} (\|\nabla \phi^{n+1}\|^2 - \|\nabla \phi^n\|^2) \\ + \frac{\theta^2}{2} (\nabla(\phi^{n+1} - \phi^n - \frac{\tau_{n+1}}{\tau_n}(\phi^n - \phi^{n-1})), \nabla(\phi^{n+1} - \phi^n)) \\ + \frac{R^{n+1} + R^n}{2R^{n+\frac{1}{2}}} \left(-\theta^2 \Delta \phi^{n+\frac{1}{2}} + F'(\phi^{n+\frac{1}{2}}) + \tilde{L}_h^\alpha \phi^{n+\frac{1}{2}}, \frac{\phi^{n+1} - \phi^n}{\tau_{n+1}}\right) = 0, \end{aligned}$$

$$\frac{|R^{n+1}|^2 - |R^n|^2}{\tau_{n+1}} = \frac{R^{n+1} + R^n}{2R^{n+\frac{1}{2}}} \left(-\theta^2 \Delta \phi^{n+\frac{1}{2}} + F'(\phi^{n+\frac{1}{2}}) + \tilde{L}_h^\alpha \phi^{n+\frac{1}{2}}, \frac{\phi^{n+1} - \phi^n}{\tau_{n+1}}\right).$$

Summing up the above two equalities, applying the identity

$$2a^{n+1}(a^{n+1} - a^n) = |a^{n+1}|^2 - |a^n|^2 + |a^{n+1} - a^n|^2,$$

and dropping some non-essential positive terms, we obtain

$$\begin{aligned} & \frac{\varepsilon^2 - \theta^2}{2} \|\nabla \phi^{n+1}\|_0^2 + \frac{\theta^2}{4} \|\nabla(\phi^{n+1} - \phi^n)\|_0^2 + |R^{n+1}|^2 \\ & - \left[ \frac{\varepsilon^2 - \theta^2}{2} \|\nabla \phi^n\|_0^2 + \frac{\theta^2}{4} \left( \frac{\tau_{n+1}}{\tau_n} \right)^2 \|\nabla(\phi^n - \phi^{n-1})\|_0^2 + |R^n|^2 \right] \\ & \leq -(\tilde{L}_l^\alpha \phi^{n+\frac{1}{2}}, \phi^{n+1} - \phi^n) = -\frac{\tilde{b}_0}{\tau_{n+1}} \|\phi^{n+1} - \phi^n\|_0^2 \leq 0. \end{aligned}$$

This completes the proof.  $\square$

The L1-CN scheme (4.1) can be efficiently implemented by following the lines similar to the first order scheme (3.9) described in the previous section.

**4.2. A second order scheme.** We first integrate the equation (3.6) and (3.5) from  $t_n$  to  $t_{n+1}$ , and multiply by  $\frac{1}{\tau_{n+1}}$  to give:

$$\begin{aligned} & \frac{1}{\tau_{n+1}} \int_{t_n}^{t_{n+1}} D_{l,t}^{\alpha,t_n} \phi dt - \frac{1}{\tau_{n+1}} \int_{t_n}^{t_{n+1}} \left[ \varepsilon^2 \Delta \phi + \left( 1 - \frac{R(t)}{R(t)} \right) \theta^2 \Delta \phi + \frac{R(t)}{R(t)} (F'(\phi) + D_{h,t}^{\alpha,t_n} \phi) \right] dt = 0, \\ & \frac{1}{\tau_{n+1}} \int_{t_n}^{t_{n+1}} \frac{dR}{dt} dt = \frac{1}{\tau_{n+1}} \int_{t_n}^{t_{n+1}} \frac{1}{2R(t)} \left( -\theta^2 \Delta \phi + F'(\phi) + D_{h,t}^{\alpha,t_n} \phi, \frac{\partial \phi}{\partial t} \right) dt, \quad n = 0, 1, \dots \quad (4.2) \end{aligned}$$

The idea is to construct second order approximations for the necessary terms involved in the above equations. We define the finite difference operators  $\hat{L}_l^\alpha$  and  $\hat{L}_h^\alpha$  by:

$$\begin{aligned} \hat{L}_l^\alpha \phi(t_{n+\frac{1}{2}}) & := \frac{1}{\tau_{n+1}} \int_{t_n}^{t_{n+1}} \left[ \frac{1}{\Gamma(1-\alpha)} \int_{t_n}^t (t-s)^{-\alpha} \frac{\phi(t_{n+1}) - \phi(t_n)}{\tau_{n+1}} ds \right] dt \\ & = \frac{\hat{b}_0}{\tau_{n+1}} \frac{\phi(t_{n+1}) - \phi(t_n)}{\tau_{n+1}}, \\ \hat{L}_h^\alpha \phi(t_{n+\frac{1}{2}}) & = \frac{1}{\tau_{n+1}} \int_{t_n}^{t_{n+1}} \left[ \sum_{k=1}^n \frac{1}{\Gamma(1-\alpha)} \int_{t_k}^{t_{k+1}} (t_{n+\frac{1}{2}} - s)^{-\alpha} \frac{\phi(t_{k+1}) - \phi(t_k)}{\tau_{k+1}} ds \right] dt \\ & = \sum_{k=0}^{n-1} \hat{b}_{n-k} \frac{\phi(t_{k+1}) - \phi(t_k)}{\tau_{k+1}}, \end{aligned}$$

where

$$\hat{b}_0 = \frac{\tau_{n+1}^{1-\alpha}}{\Gamma(3-\alpha)}, \quad \hat{b}_{n-k} = \frac{1}{\Gamma(1-\alpha)\tau_{n+1}} \int_{t_n}^{t_{n+1}} \int_{t_k}^{t_{k+1}} (t-s)^{-\alpha} ds dt, \quad k = 0, 1, \dots, n-1.$$

We want to use these two operators to approximate the local term  $\frac{1}{\tau_{n+1}} \int_{t_n}^{t_{n+1}} D_{l,t}^{\alpha,t_n} dt$  and the history term  $\frac{1}{\tau_{n+1}} \int_{t_n}^{t_{n+1}} D_{h,t}^{\alpha,t_n} dt$  respectively. Note that a similar operator without splitting, called  $L1^+$  formula, has been used in [22] to approximate the Caputo fractional derivative, and the resulting scheme has been numerically found to be second order accurate. However, there is no available analysis for the truncation error, nor for the stability.

Applying  $\widehat{L}_l^\alpha \phi(t_{n+\frac{1}{2}})$  and  $\widehat{L}_h^\alpha \phi(t_{n+\frac{1}{2}})$  to approximate  $\frac{1}{\tau_{n+1}} \int_{t_n}^{t_{n+1}} D_{l,t}^{\alpha,t_n} dt$  and  $\frac{1}{\tau_{n+1}} \int_{t_n}^{t_{n+1}} D_{h,t}^{\alpha,t_n} dt$  respectively, and trapezoidal formula to approximate the remaining terms in (4.2), we arrive at the following  $L1^+$ -CN scheme:

$$\begin{aligned} \widehat{L}_l^\alpha \phi^{n+\frac{1}{2}} - \varepsilon^2 \frac{\Delta(\phi^{n+1} + \phi^n)}{2} + \left(1 - \frac{R^{n+1} + R^n}{2R^{n+\frac{1}{2}}}\right) \theta^2 \Delta \phi^{n+\frac{1}{2}} \\ + \frac{R^{n+1} + R^n}{2R^{n+\frac{1}{2}}} \left(F'(\phi^{n+\frac{1}{2}}) + \widehat{L}_h^\alpha \phi^{n+\frac{1}{2}}\right), \end{aligned} \quad (4.3a)$$

$$\frac{R^{n+1} - R^n}{\tau_{n+1}} = \frac{1}{2R^{n+\frac{1}{2}}} \left(-\theta^2 \Delta \phi^{n+\frac{1}{2}} + F'(\phi^{n+\frac{1}{2}}) + \widehat{L}_h^\alpha \phi^{n+\frac{1}{2}}, \frac{\phi^{n+1} - \phi^n}{\tau_{n+1}}\right), \quad (4.3b)$$

where  $\phi^{n+\frac{1}{2}} := \phi^n + \frac{\tau_{n+1}}{2\tau_n}[\phi^n - \phi^{n-1}]$  and  $R^{n+\frac{1}{2}} := R^n + \frac{\tau_{n+1}}{2\tau_n}[R^n - R^{n-1}]$  are the explicit approximation to  $\phi(t_{n+\frac{1}{2}})$  and  $R(t_{n+\frac{1}{2}})$ , respectively.

We leave the error estimation as an open question, but present the stability result for the scheme in the following theorem.

**Theorem 4.2.** *For the  $L1^+$ -CN scheme (4.3), it holds*

$$\begin{aligned} \frac{\varepsilon^2 - \theta^2}{2} \|\nabla \phi^{n+1}\|_0^2 + \frac{\theta^2}{4} \|\nabla(\phi^{n+1} - \phi^n)\|_0^2 + |R^{n+1}|^2 \\ - \left[ \frac{\varepsilon^2 - \theta^2}{2} \|\nabla \phi^n\|_0^2 + \frac{\theta^2}{4} \left(\frac{\tau_{n+1}}{\tau_n}\right)^2 \|\nabla(\phi^n - \phi^{n-1})\|_0^2 + |R^n|^2 \right] \\ \leq -\frac{\widehat{b}_0}{\tau_{n+1}} \|\phi^{n+1} - \phi^n\|_0^2 \leq 0, \quad n = 0, 1, \dots \end{aligned}$$

This implies that the scheme is unconditionally stable in the cases of the uniform mesh or  $\theta = 0$ .

*Proof.* The proof is very similar to Theorem 4.1, we leave it to interested readers.  $\square$

**Remark 4.1.** *One can also reformulate the original equation (3.1) into the following equivalent form:*

$$D_{l,t}^{\alpha,t_n} \phi - \varepsilon^2 \Delta \phi + \left(1 - \frac{R(t)}{\sqrt{\overline{E}_\theta(\phi) + C_0}}\right) \theta^2 \Delta \phi + \frac{R(t)}{\sqrt{\overline{E}_\theta(\phi) + C_0}} \left(F'(\phi) + D_{h,t}^{\alpha,t_n} \phi\right) = 0, \quad (4.4a)$$

$$\frac{dR}{dt} = \frac{1}{2\sqrt{\overline{E}_\theta(\phi) + C_0}} \left(-\theta^2 \Delta \phi + F'(\phi) + D_{h,t}^{\alpha,t_n} \phi, \frac{\partial \phi}{\partial t}\right), \quad t \in [t_n, t_{n+1}], n = 0, 1, \dots \quad (4.4b)$$

Starting with this equivalent system and following the discussion in the above sections, it is also possible to construct unconditionally stable schemes based on  $L1$ ,  $L1$ -CN and  $L1^+$ -CN formula for the discretization of the fractional derivatives. However, compared to the schemes constructed for the reformulation (3.5)-(3.6), a drawback using (4.4) is that one has to compute  $\overline{E}_\theta^n$  or  $\overline{E}_\theta^{n+\frac{1}{2}}$ , which is more expensive than computing  $R^n$  or  $R^{n+\frac{1}{2}}$ . Remember that  $\overline{E}_\theta^{n+\frac{1}{2}}$  is an explicit approximation to  $\overline{E}_\theta(\phi(t_{n+\frac{1}{2}}))$  involving the nonlocal terms  $F_h(t_n, t_{n+\frac{1}{2}}; \phi) + \sum_{k=1}^{n-1} F_h(t_k, t_{k+1}; \phi)$ . It is notable that the new SAV approach developed recently in [7, 8] may be applied to deal with

the nonlinear term and the history part of the fractional derivative. Then energy stable schemes can be constructed based on the following reformulation:

$$D_{l,t}^{\alpha,t_n} \phi - \varepsilon^2 \Delta \phi + (1 - \eta(t)) \theta^2 \Delta \phi + \eta(t) (F'(\phi) + D_{h,t}^{\alpha,t_n} \phi) = 0,$$

$$\frac{d\bar{E}_\theta(\phi)}{dt} = \eta(t) \left( -\theta^2 \Delta \phi + F'(\phi) + D_{h,t}^{\alpha,t_n} \phi, \frac{\partial \phi}{\partial t} \right),$$

where the scalar auxiliary function  $\eta(t)$  is a Lagrange multiplier with  $\eta(0) = 1$ .

## 5. NUMERICAL RESULTS

This section is devoted to numerical investigation of the proposed schemes in terms of the accuracy and stability. For the comparison purpose, we will repeat most of the numerical examples in our previous work [20]. In the following examples, we always set  $\theta = 0$  and  $C_0 = 0$  in the schemes unless specified otherwise. The spatial discretization is the Fourier method or Legendre Galerkin spectral method using numerical quadratures. In order to test the accuracy of the proposed schemes, the error is measured by the maximum norm, i.e.,  $\max_{1 \leq n \leq M} \|\phi^n - \phi(t_n)\|_\infty$  or  $\max_{1 \leq n \leq M} \|\phi_M^n - \phi_{2M}^{2n}\|_\infty$ , the latter norm will be used when the exact solution is not available. In order to reduce the computational complexity, a fast evaluation technique based on the sum-of-exponentials approach [23, 38] is used to calculate the history part  $D_{h,t}^{\alpha,t_n}$  of the time fractional derivative.

### 5.1. Convergence order test.

**Example 5.1.** Consider the following fractional Allen-Cahn equation:

$${}_0D_t^\alpha \phi - \varepsilon^2 \Delta \phi - \phi(1 - \phi^2) = s, \quad (\mathbf{x}, t) \in (0, 2\pi)^2 \times (0, T],$$

subject to the periodic boundary condition, where  $s(\mathbf{x}, t)$  is a fabricated source term such that the exact solution is

$$\phi(\mathbf{x}, t) = 0.2t^5 \sin(x) \cos(y).$$

The Fourier spectral method with  $128 \times 128$  modes is used to discretize the equations in space. It has been checked that this Fourier mode number is large enough so that the spatial discretization error is negligible compared to the temporal discretization. We present in Figure 1 the error as functions of the time step sizes in log-log scale with  $T = 1$ . It is observed, as expected, that the L1 scheme (3.12), L1-CN scheme (4.1), and L1<sup>+</sup>-CN scheme (4.3) achieve respectively the first order,  $2 - \alpha$  order, and second order convergence for all tested  $\alpha$ .

**Example 5.2.** Consider the same equation as in Example 5.1, but with the Neumann boundary condition, and the exact solution

$$\phi(\mathbf{x}, t) = 0.2(t^\mu + 1) \cos(\pi x) \cos(\pi y), \quad (\mathbf{x}, t) \in (-1, 1)^2 \times (0, T],$$

which has limited regularity at the initial time  $t = 0$ .

In this test, a Legendre Galerkin spectral method with polynomials of degree 32 in each spatial direction is used for the spatial discretization. The purpose of this test is to not only verify the convergence rate of the schemes, but also investigate the impact of the regularity on the accuracy.

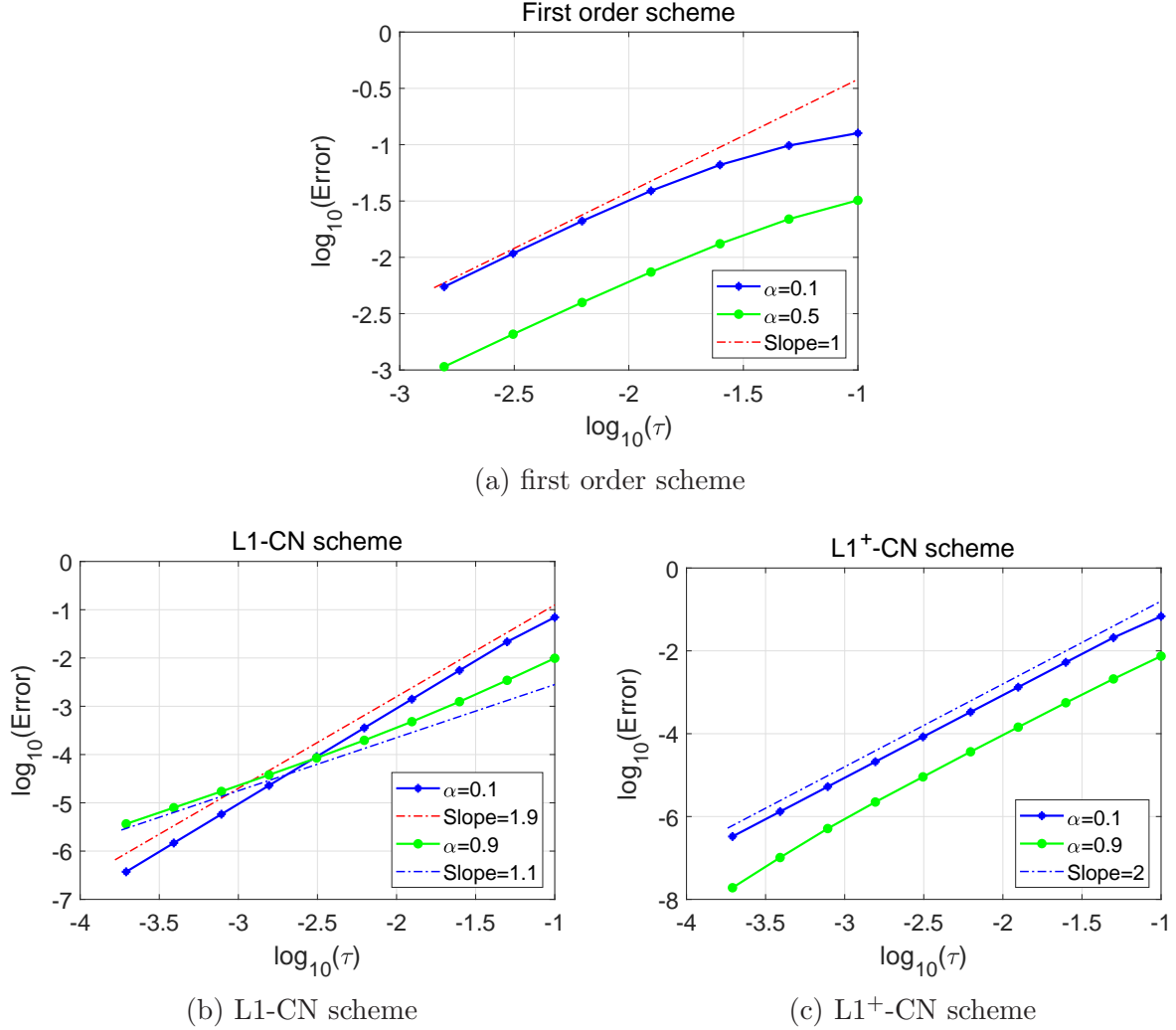
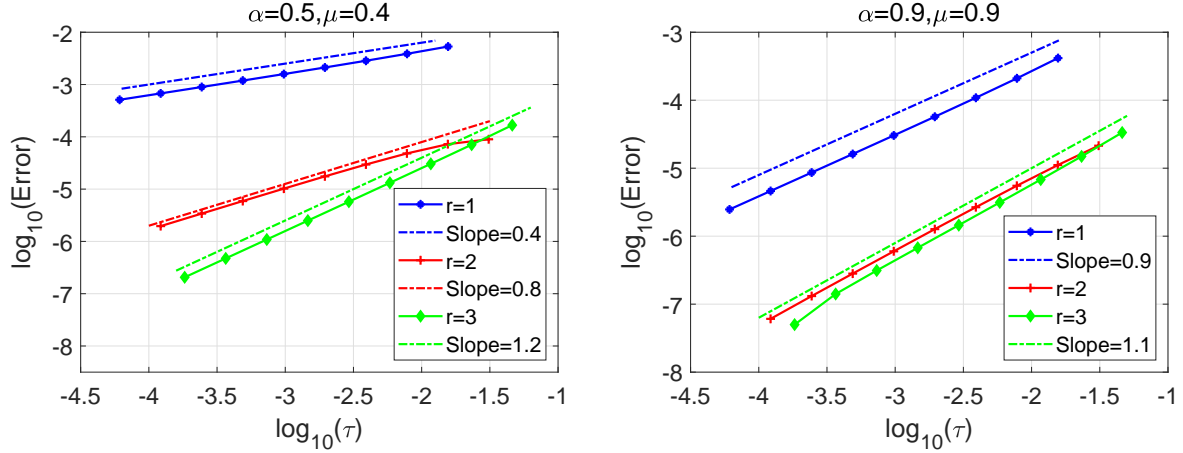


FIGURE 1. (Example 5.1) Error decay versus the time step sizes for the first order scheme, L1-CN scheme, and L1<sup>+</sup>-CN scheme with several different  $\alpha$ .

In particular, we are interested in studying the impact of the graded mesh parameter  $r$  on the convergence rate. It will help us to choose the optimal value of  $r$  to recover the convergence rate of the proposed schemes for low regular solutions. The calculation is performed by using the L1-CN scheme (4.1) and L1<sup>+</sup>-CN scheme (4.3) with  $M = 64 \times 2^k, k = 1, 2, \dots, 9$ . In Figure 2, we plot the  $L^\infty$  errors in log-log scale with respect to the maximum time step size, i.e.,  $\tau = t_M - t_{M-1}$ . The presented results are in a perfect agreement with the expected convergence rates, i.e.,  $\min\{\mu r, 2 - \alpha\}$  order for the L1-CN scheme, and  $\min\{\mu r, 2\}$  order for the L1<sup>+</sup>-CN scheme. This suggests use of the graded mesh with  $r = \frac{2-\alpha}{\mu}$  for the L1-CN scheme and  $r = \frac{2}{\mu}$  for the L1<sup>+</sup>-CN scheme. Doing so the schemes reach the optimal convergence rates for solutions of this class.



(a) L1-CN scheme

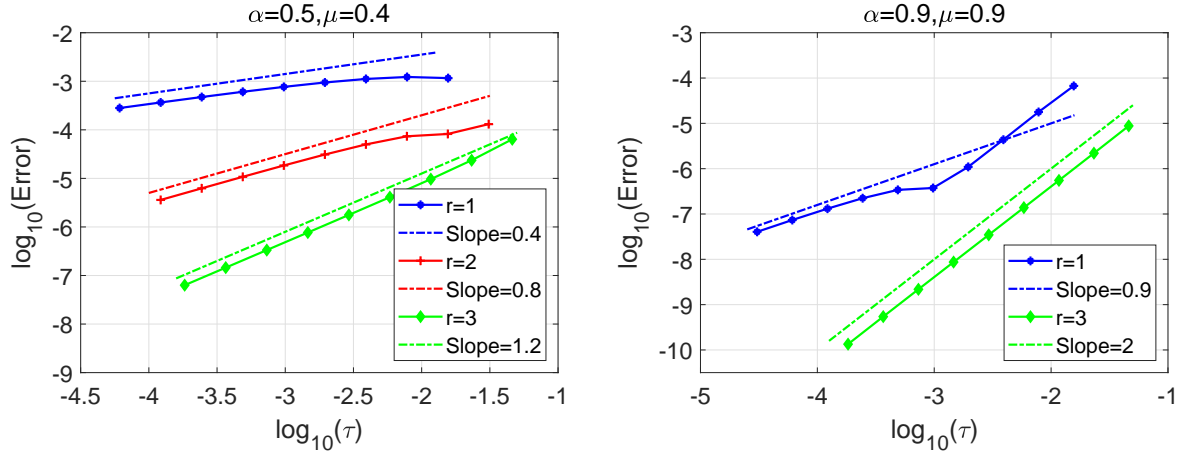
(b) L1<sup>+</sup>-CN scheme

FIGURE 2. (Example 5.2) Error history for the L1-CN scheme and L1<sup>+</sup>-CN scheme for different values of the mesh parameter  $r$  and fractional derivative order  $\alpha$ : the first line corresponds to L1-CN scheme; the second line is for L1<sup>+</sup>-CN scheme.

**Example 5.3.** Consider the fractional Allen-Cahn Neumann problem in the domain  $(-1, 1) \times (-1, 1)$  with the initial condition  $\phi(\mathbf{x}, 0) = \cos(4\pi x) \cos(4\pi y)$  without a source term. The exact solution is unavailable.

The spatial discretization uses the Legendre spectral method with high enough mode number to avoid possible spatial error contamination. Since the exact solution is unknown, the error of the numerical solution is defined as:

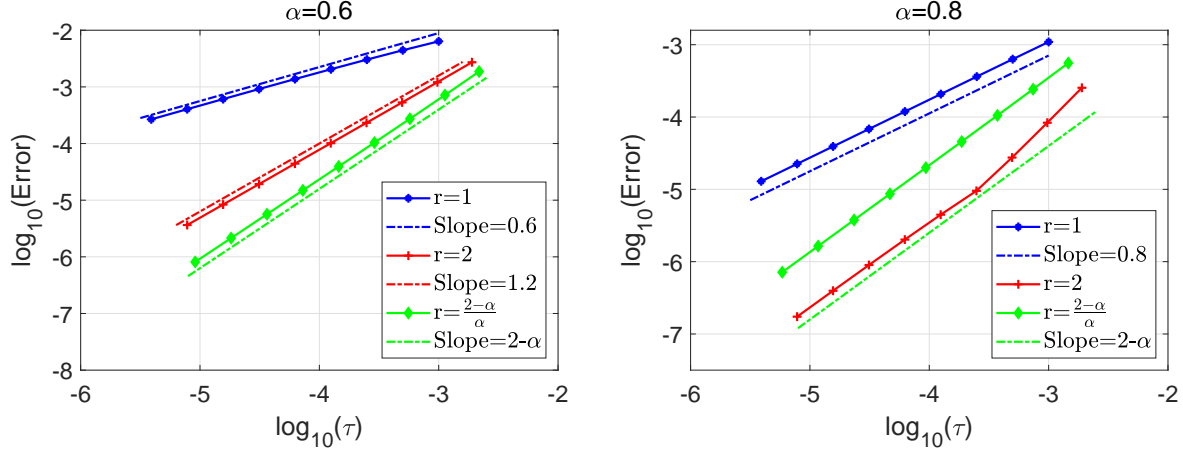
$$e(\tau) = \max_{1 \leq n \leq M} \|\phi_M^n - \phi_{2M}^{2n}\|_\infty$$

It is known that the time fractional operator creates some kind of singularity at the initial time, and the solution behaves like  $t^\alpha$  with respect to the time variable; see, e.g., [11] for a numerical confirmation of this behavior. In this example, we will take a closer look at the

initial error to investigate how the initial low regularity affects the accuracy of the computed solutions. We also study the impact of the mesh ratio  $r$  on the convergence order. The calculation is run up  $T = 0.01$  using graded mesh with grid points  $M$  ranging from 20 to  $10 \times 2^{10}$ . In Figure 3, we present the errors in log-log scale with respect to the maximum mesh size, i.e.,  $\tau = \max_{1 \leq n \leq M} (t_n - t_{n-1}) = t_M - t_{M-1}$ . It is observed in the figure that the L1-CN scheme (4.1) and L1<sup>+</sup>-CN scheme (4.3) attain the convergence rate  $\min\{\alpha r, 2 - \alpha\}$  and  $\min\{\alpha r, 2\}$  respectively for all tested  $\alpha$  and  $r$ . Clearly the optimal  $r$  is  $\frac{2-\alpha}{\alpha}$  for the scheme (4.1) and  $\frac{2}{\alpha}$  for the scheme (4.3). In these cases, both schemes reach the theoretical convergence order, i.e.,  $2 - \alpha$  order and second order respectively. For the uniform mesh, i.e.,  $r = 1$ , the schemes lose the optimal convergence order. This is indicative that the regularity of the solution is lower than what the theoretical convergence order of the schemes requests.

The stability of the proposed schemes is investigated through running the calculation with  $\varepsilon^2 = 0.001$  for long time, i.e.,  $T = 50$ , using a time step size as large as possible. In view of the singularity feature at the beginning time, we split the interval  $[0, T]$  into two subintervals  $[0, 1]$  and  $(1, T]$ . We compute the solution using the graded mesh with optimal  $r$  in  $[0, 1]$ , and using the uniform mesh with the time step size  $\Delta t$  in  $(1, T]$ . The computed modified energies and original energy are presented in Figure 4. The modified energies shown in the left figures exhibits dissipative features during the running time even if a large time step size  $\Delta t = 1$  is used. This demonstrates good stability and modified energy dissipation properties of the schemes proved in Theorems 4.1 and 4.2. However, as shown in the right figures, the original energy is dissipative only for relatively small time step size. Precisely, the original energy fails to keep dissipation during some time period for the solution computed with  $\Delta t = 1$ . It is noteworthy that this failure is not due to the instability of the schemes, but due to possible large error caused by the use of the large time step size. Another notable fact is that all the original energy curves coincide with each other for the time step sizes ranging from 0.0001 to 0.1. In fact the computed original energy is a key indication of the efficiency of the numerical methods for phase field models. The observed dissipation feature of the original energy signifies that the solution evolves in the right way, which is important for long time simulation. The last point we want to emphasize is that although the time step size  $\Delta t = 1$  was not able to produce correct original energy dissipation, use of larger  $\Delta t$  is still possible through an adaptive strategy. That is, adaptively utilize larger  $\Delta t$  during the time period when the phase transition is slow. Doing so will benefit the most from the unconditional stability of the proposed schemes.

**5.2. Order sensibility of a benchmark problem.** In this test case, we intend to apply the proposed schemes to the interface moving problem governed by the fractional Allen-Cahn equation in the domain  $(-32, 32) \times (-32, 32)$ . The initial state of the interface is the circle of the radius  $R_0 = 8$ . It is known that the circle interface will shrink and eventually disappear due to the driving force. This problem was also studied in [20] to verify the performance of the scheme proposed in that paper. In the classical case, i.e.,  $\alpha = 1$ , it was shown [5, 39] that the radius  $R(t)$  of the circle at the given time  $t$  evolves as  $R(t) = \sqrt{R_0^2 - 2t}$ . That is, the ratio is monotonously decreasing and vanishes at  $T = 32$ . This problem has been frequently served as a benchmark to test the efficiency of the numerical methods.



(a) L1-CN scheme

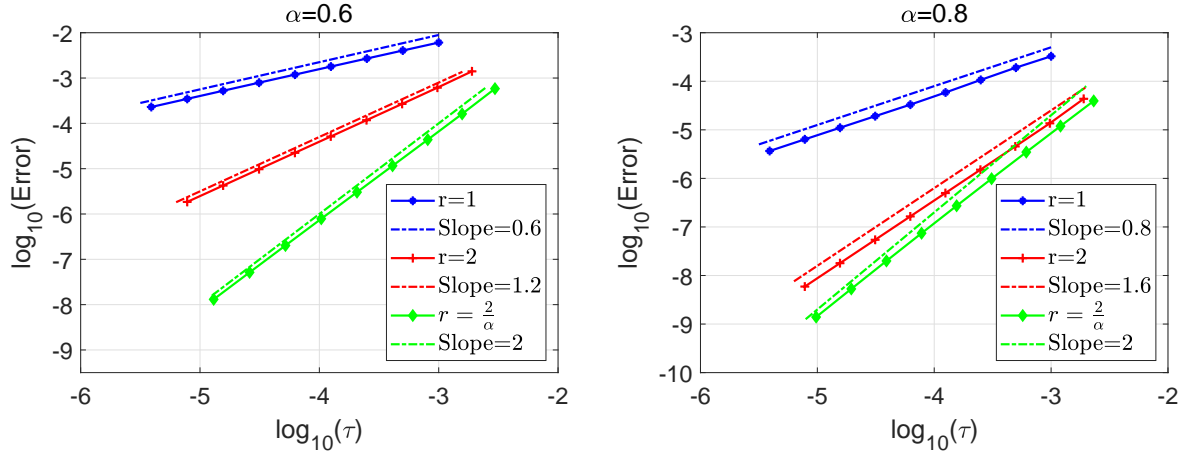
(b) L1<sup>+</sup>-CN scheme

FIGURE 3. (Example 5.3) Effect of the graded mesh parameter  $r$  on the convergence rate of the L1-CN scheme (the first line) and L1<sup>+</sup>-CN scheme (the second line) with  $\varepsilon^2 = 0.01$ .

The problem is discretized by the L1-CN time stepping scheme using the graded mesh with  $r = \frac{2-\alpha}{\alpha}$  in the subinterval  $[0, 1]$  and the uniform mesh in the subinterval  $(1, T]$ . The Legendre spectral method in space uses polynomials of degree 128 in each direction. For comparison purposes the computation is performed with the same meshes for the same fractional orders  $\alpha$  as in [20]. The computed interface evolution is shown in Figure 5. The computed  $R^2$  and the free energy  $E(\phi^n)$  versus the time are also plotted in Figure 6. The interface movement shown in Figure 5 is almost the same compared to the results reported in [20]. The agreement on  $R^2$  and  $E(\phi)$  between the current scheme and the one in [20] can be observed equally. This demonstrates the efficiency of the both methods proposed in [20] and in the present paper. However, as we have already emphasized, the novelty of present work is the rigorous proof of an energy dissipation law,

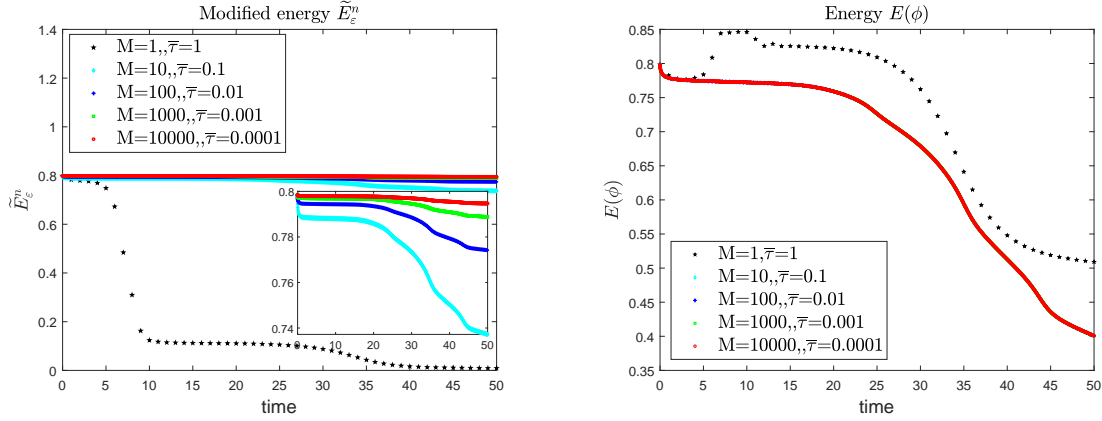
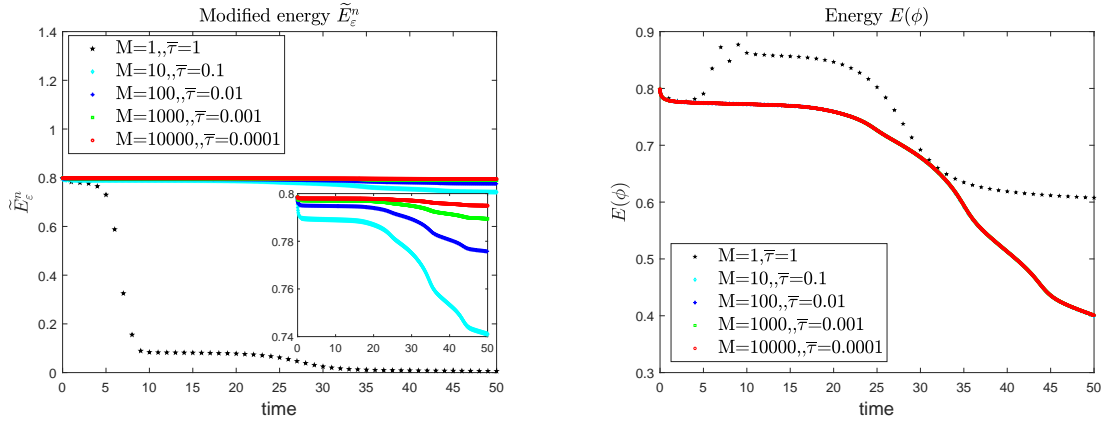
(a) L1-CN scheme with  $\alpha = 0.6$ (b) L1<sup>+</sup>-CN scheme with  $\alpha = 0.6$ 

FIGURE 4. (Example 5.3) Evolution in time of the modified energy and original energy computed by using different time step sizes.

both in the continuous and discrete cases, not only in the uniform mesh but also in the graded mesh.

**5.3. Coarsening dynamics.** Finally we test the L1<sup>+</sup>-CN scheme (4.3) to the two-phase coarsening problem, by solving the fractional Allen-Cahn equation with  $\varepsilon^2 = 0.001$  in  $(-1, 1)^2$ . The initial condition is a random data, same as used in [20]. The simulation is performed in the graded mesh with  $r = \frac{2}{\alpha}$ ,  $M = 100$  in  $[0, 1]$  and the uniform mesh with time step size  $\Delta t = 0.01$  in  $(1, T]$ . The spatial spectral approximation uses  $128 \times 128$  basis functions. Figure 7 presents some snapshots of the simulated phase function and the computed free energy  $E(\phi)$  versus time for a number of fractional orders  $\alpha = 1, 0.9, 0.7$ , and  $0.5$ . It is observed that the results are not sensitive to the fractional orders at the early stage as there is no distinguishable difference on the isoline plots among different fractional orders before  $t = 5$ . After that, the solutions apparently

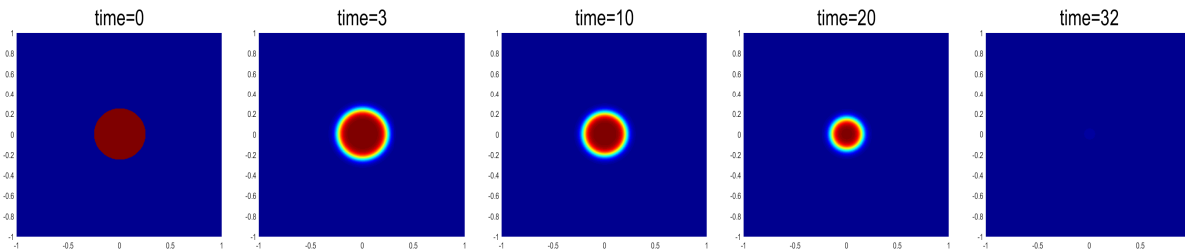
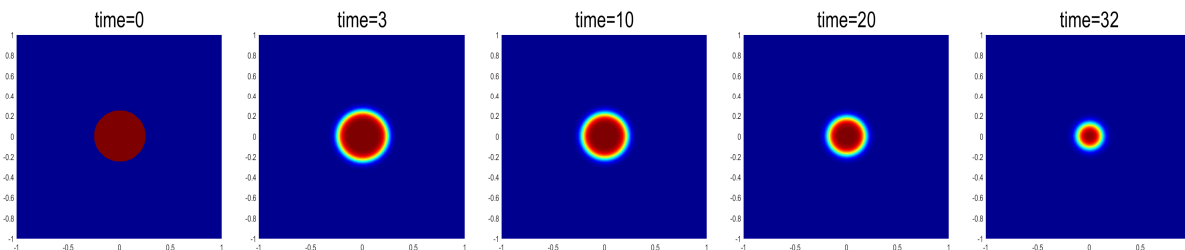
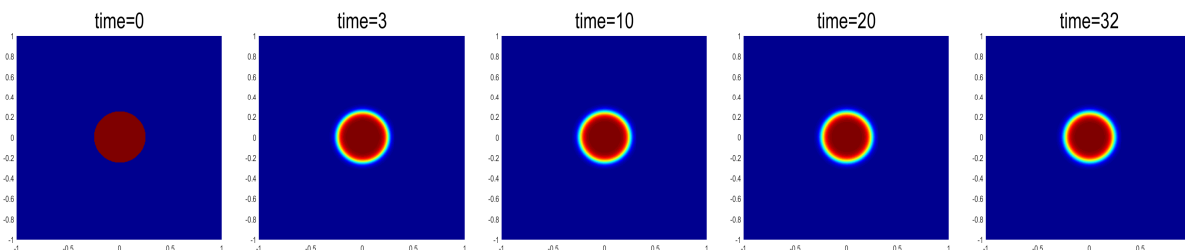
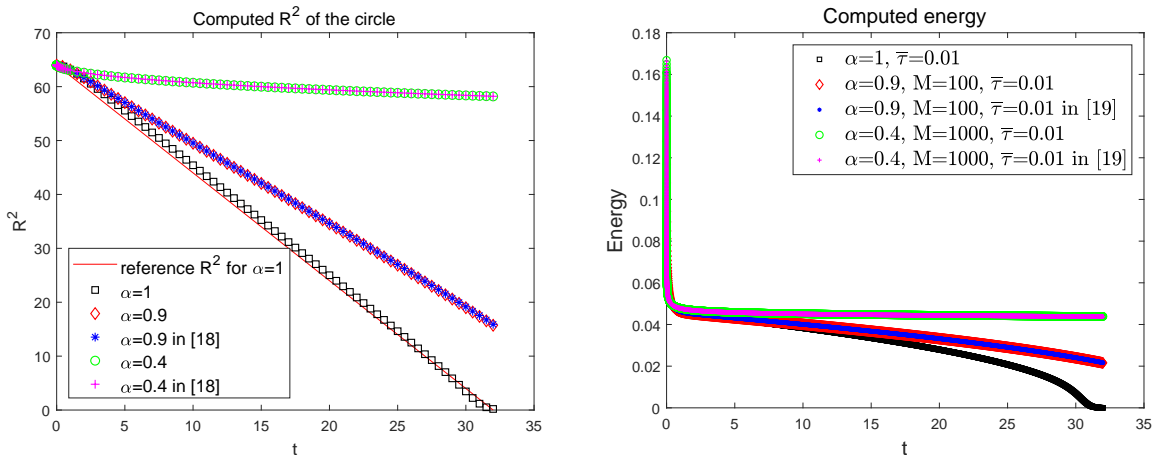
(a)  $\alpha = 1$  and  $\Delta t = 0.01$ (b)  $\alpha = 0.9$ ,  $M = 100$ , and  $\Delta t = 0.01$ (c)  $\alpha = 0.4$ ,  $M = 1000$ , and  $\Delta t = 0.01$ 

FIGURE 5. Snapshots of the interface evolution simulated by using the L1-CN scheme with  $C_0 = 1000$  for  $\alpha = 1, 0.9$ , and  $0.4$ .

start to deviate, and develop into long time phase coarsening. Note that similar results and interpretation of these results have been presented in [20]. The computed free energy  $E(\phi^n)$  shown in the last row figures is also in a good agreement with the result reported in [20].

## 6. CONCLUDING REMARKS

We have proposed a class of energy dissipative schemes for the time fractional Allen-Cahn equation. The construction of the schemes made use of a new idea to reformulate the original equation. By splitting the time fractional derivative into a local part and a history part, and adding the history part to the new defined energy, a dissipation law for the new energy can be established in any given time grid. Based on this splitting and an auxiliary variable approach, several schemes of different convergence orders were constructed by combining the L1 and L1<sup>+</sup> discretizations to the time fractional derivative and Crank-Nicolson formula to other necessary terms. The main property of the proposed schemes is its unconditional stability for general



(a) Interface radius as functions of the time.

(b) Free energy dissipation.

FIGURE 6. Comparison of the computed  $R^2$  and total free energy computed between the L1-CN scheme and the scheme in [20].

meshes. The proved stability of the schemes built on the graded mesh is of particular interesting because this type of mesh has been found very useful to treat with the starting point singularity of the time fractional differential equations. Moreover the splitting-based approach allows use of the sum-of-exponentials technique to fast evaluate the history part of the fractional derivative without affecting the stability property of the schemes. The efficiency of the proposed method was verified by a series of numerical experiments. the authors proved that the fractional derivative of the traditional free energy is always nonpositive.

It is notable that there exist some similar dissipation laws for memorized or mean energy, and different energy laws lead to SAV-based schemes having quite different stability properties. It seems to us that the energy dissipation law established in the current paper facilitates construction of high order stable schemes. It is also worth to mention that the idea of the present work is most likely extendable to some other gradient flows, such as the Cahn-Hilliard equation and molecular beam epitaxial growth models.

## REFERENCES

- [1] M. Ainsworth and Z. Mao. Analysis and approximation of a fractional Cahn-Hilliard equation. *SIAM J. Numer. Anal.*, 55(4):1689–1718, 2017.
- [2] M. Ainsworth and Z. Mao. Well-posedness of the Cahn-Hilliard equation with fractional free energy and its Fourier Galerkin approximation. *Chaos Soliton. Fract.*, 102:264–273, 2017.
- [3] G. Akagi, G. Schimperna, and A. Segatti. Fractional Cahn-Hilliard, Allen-Cahn and porous medium equations. *J. Differ. Equations*, 261(6):2935–2985, 2016.
- [4] D. M. Anderson, G. B. Mcfadden, and A. A. Wheeler. Diffuse-interface methods in fluid mechanics. *Annu. Rev. Fluid Mech.*, 30:139–165, 1997.
- [5] L. Chen and J. Shen. Applications of semi-implicit Fourier-spectral method to phase field equations. *Comput. Phys. Commun.*, 108(2-3):147–158, 1998.

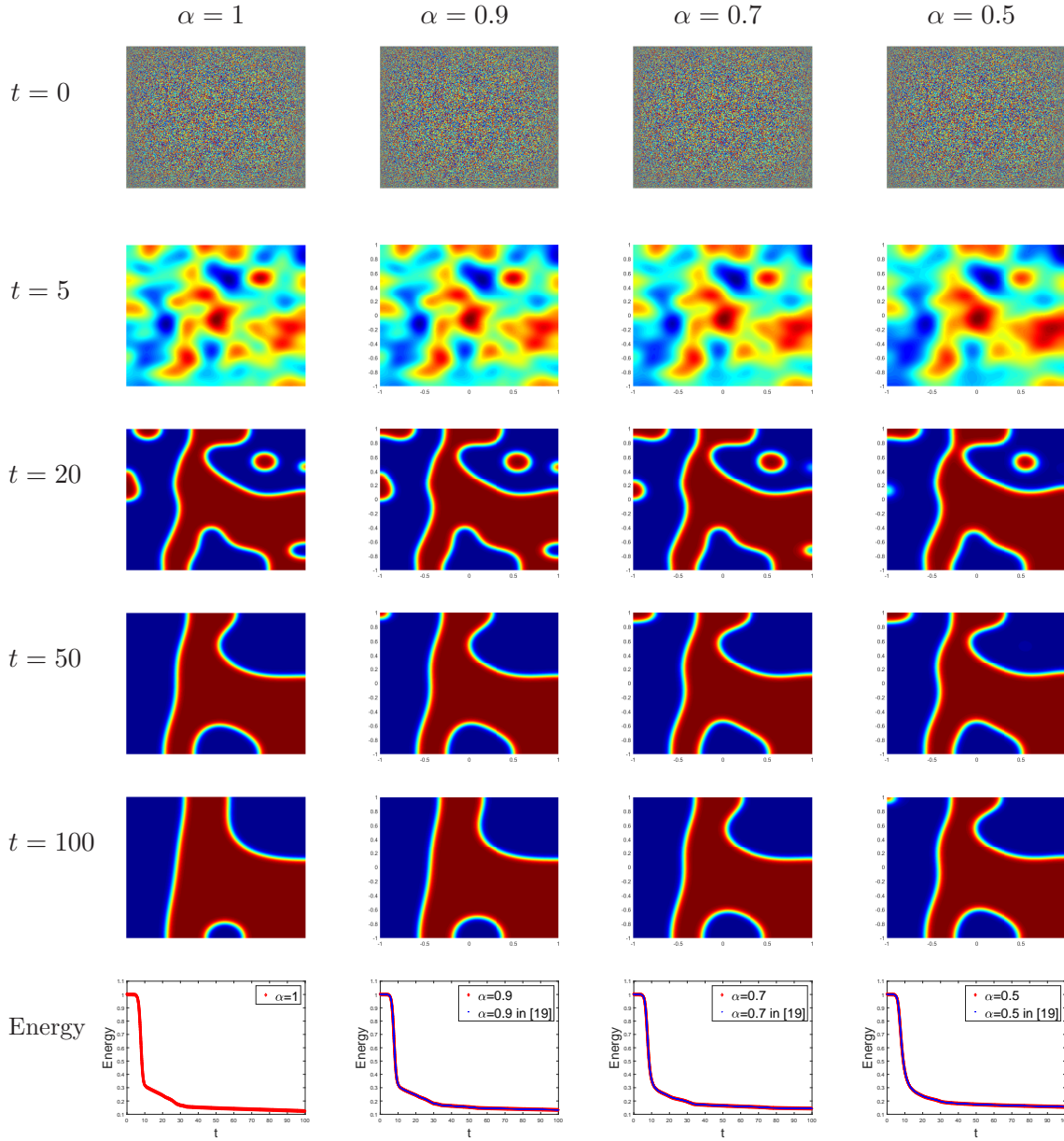


FIGURE 7. Snapshots of the simulated phase field evolution starting with a random initial data for  $\alpha = 1, 0.9, 0.7, 0.5$  (the first five rows); Comparisons of the computed energy between the L1<sup>+</sup>-CN scheme and the scheme in [20].

- [6] L. Chen, J. Zhao, W. Cao, H. Wang, and J. Zhang. An accurate and efficient algorithm for the time-fractional molecular beam epitaxy model with slope selection. *Comput. Phys. Commun.*, 2018.
- [7] Q. Cheng, C. Liu, and J. Shen. A new Lagrange multiplier approach for gradient flows. *Comput. Methods Appl. Mech. Engrg.*, 367:113070, 2020.

- [8] Q. Cheng and J. Shen. Global constraints preserving scalar auxiliary variable schemes for gradient flows. *SIAM J. Sci. Comput.*, 42(4):A2489–A2513, 2020.
- [9] M. Doi and S. F. Edwards. *THE THEORY OF POLYMER DYNAMICS*. Clarendon Press, 1986.
- [10] Q. Du, L. Ju, X. Li, and Z. Qiao. Stabilized linear semi-implicit schemes for the nonlocal Cahn-Hilliard equation. *J. Comput. Phys.*, 363:39–54, 2018.
- [11] Q. Du, J. Yang, and Z. Zhou. Time-fractional Allen-Cahn equations: analysis and numerical methods. *arXiv:1906.06584v1*, pages 1–24, 2019.
- [12] K. R. Elder and M. Grant. Modeling elastic and plastic deformations in nonequilibrium processing using phase field crystals. *Phys. Rev. E*, 70(5):051605, 2004.
- [13] K. R. Elder, M. Katakowski, M. Haataja, and M. Grant. Modeling elasticity in crystal growth. *Phys. Rev. Lett.*, 88(24):245701, 2002.
- [14] K. R. Elder, N. Provatas, J. Berry, P. Stefanovic, and M. Grant. Phase-field crystal modeling and classical density functional theory of freezing. *Phys. Rev. B*, 75(6):794–802, 2007.
- [15] J. Fraaije. Dynamic density functional theory for microphase separation kinetics of block copolymer melts. *J. Chem. Phys.*, 99(11):9202–9212, 1993.
- [16] J. Fraaije and G. Sevink. Model for pattern formation in polymer surfactant nanodroplets. *Macromolecules*, 36(21):7891–7893, 2003.
- [17] L. Giacomelli and F. Otto. Variational formulation for the lubrication approximation of the hele-shaw flow. *Calc. Var. Partial Dif.*, 2001.
- [18] M. E. Gurtin and D. Polignone. Two-phase binary fluids and immiscible fluids described by an order parameter. *Math. Models Methods Appl. Sci.*, 6:815–831, 1996.
- [19] D. Hou, M. Azaiez, and C. Xu. A variant of scalar auxiliary variable approaches for gradient flows. *J. Comput. Phys.*, 395:307–332, 2019. <https://doi.org/10.1016/j.jcp.2019.05.037>.
- [20] D. Hou, H. Zhu, and C. Xu. Highly efficient schemes for time fractional Allen-Cahn equation using extended SAV approach. *arXiv:1910.09087*, pages 1–28, 2019.
- [21] B. Ji, H. Liao, Y. Gong, and L. Zhang. Adaptive linear second-order energy stable schemes for time-fractional Allen-Cahn equation with volume constraint. *Commun. Nonlinear Sci. Numer. Simulat.*, 90:105366, 2020.
- [22] B. Ji, H. Liao, Y. Gong, and L. Zhang. Adaptive second-order Crank-Nicolson time-stepping schemes for time-fractional molecular beam epitaxial growth models. *SIAM J. Sci. Comput.*, 42(3):B738–B760, 2020.
- [23] S. Jiang, J. Zhang, Q. Zhang, and Z. Zhang. Fast evaluation of the Caputo fractional derivative and its applications to fractional diffusion equations. *Commun. Comput. Phys.*, 21(3):650–678, 2017.
- [24] R. Larson. Arrested tumbling in shearing flows of liquid-crystal polymers. *Macromolecules*, 23(17):3983–3992, 1990.
- [25] R. Larson and H. Öttinger. Effect of molecular elasticity on out-of-plane orientations in shearing flows of liquid-crystalline polymers. *Macromolecules*, 24(23):6270–6282, 1991.
- [26] F. Leslie. Theory of Flow Phenomena in Liquid Crystals. *Advances in Liquid Crystals*, 4:1–81, 1979.
- [27] Z. Li, H. Wang, and D. Yang. A space-time fractional phase-field model with tunable sharpness and decay behavior and its efficient numerical simulation. *J. Comput. Phys.*, 347:20–38, 2017.

- [28] Y. Lin and C. Xu. Finite difference/spectral approximations for the time-fractional diffusion equation. *J. Comput. Phys.*, 225(2):1533–1552, 2007.
- [29] H. Liu, A. Cheng, H. Wang, and J. Zhao. Time-fractional Allen-Cahn and Cahn-Hilliard phase-field models and their numerical investigation. *Comput. Math. Appl.*, 76:1876–1896, 2018.
- [30] F. Otto. Lubrication approximation with prescribed nonzero contact angle. *Commun. Part. Diff. Eq.*, 1998.
- [31] C. Quan, T. Tang, and J. Yang. How to define dissipation-preserving energy for time-fractional phase-field equations. *CSIAM Trans. Appl. Math.*, 1(3):478–490, 2020.
- [32] C. Quan, T. Tang, and J. Yang. Numerical energy dissipation for time-fractional phase-field equations. *arXiv:2009.06178*, pages 1–22, 2020.
- [33] J. Shen, J. Xu, and J. Yang. The scalar auxiliary variable (SAV) approach for gradient flows. *J. Comput. Phys.*, 353:407–416, 2018.
- [34] J. Shen, J. Xu, and J. Yang. A new class of efficient and robust energy stable schemes for gradient flows. *SIAM Rev.*, 61(3):474–506, 2019.
- [35] Jie Shen, Jie Xu, and Jiang Yang. The scalar auxiliary variable (SAV) approach for gradient flows. *Journal of Computational Physics*, 353:407–416, 2018.
- [36] F. Song, C. Xu, and G. Em Karniadakis. A fractional phase-field model for two-phase flows with tunable sharpness: Algorithms and simulations. *Comput. Methods Appl. Mech. Engrg.*, 305:376–404, 2016.
- [37] T. Tang, H. Yu, and T. Zhou. On energy dissipation theory and numerical stability for time-fractional phase field equations. *SIAM J. Sci. Comput.*, 41(6):A3757–A3778, 2019.
- [38] Y. Yan, Z. Sun, and J. Zhang. Fast evaluation of the caputo fractional derivative and its applications to fractional diffusion equations: A second-order scheme. *Commun. Comput. Phys.*, 22(4):1028–1048, 2017.
- [39] X. Yang. Linear, first and second-order, unconditionally energy stable numerical schemes for the phase field model of homopolymer blends. *J. Comput. Phys.*, 327:294–316, 2016.
- [40] P. Yue, J. Feng, C. Liu, and J. Shen. A diffuse-interface method for simulating two-phase flows of complex fluids. *J. Fluid Mech.*, 515:293–317, 2004.
- [41] J. Zhao, L. Chen, and H. Wang. On power law scaling dynamics for time-fractional phase field models during coarsening. *Commun. Nonlinear Sci. Numer. Simulat.*, 70:257–270, 2019.
- [42] G. Zhen, J. Lowengrub, C. Wang, and S. Wise. Second order convex splitting schemes for periodic nonlocal Cahn-Hilliard and Allen-Cahn equations. *J. Comput. Phys.*, 277:48–71, 2014.